

Real-Time Visualization of G2L4 Reverse Transcriptase in DNA Repair via Microhomology-Mediated End Joining

Pangmiaomiao Zhang¹, Mo Guo², Y. Jessie Zhang², Alan M. Lambowitz^{2,3}, and Yi-Chih Lin^{1,*}

¹ Department of Chemistry, University of Texas at Austin, United States

² Department of Molecular Biosciences, University of Texas at Austin, United States

³ Department of Medicine / Oncology, University of Texas at Austin, United States

*Correspondence to: Yi-Chih Lin (yichih.lin@utexas.edu)

This PDF includes:

Materials and Methods

G2L4 RT Expression and Purification	2
Factor Xa Cleavage of the N-terminal MBP Tag	2
MMEJ Substrate Preparation	2
HS-AFM Imaging	2
Image Processing and Data Analysis	2

Supplementary Tables

Table S1. MMEJ substrate sequence	4
Table S2. Experimental conditions of HS-AFM experiments	4

Supplementary Figures

Figure S1. Structural dynamics of a G2L4 RT dimer in APO condition.	5
Figure S2. Relative percentage of MMEJ dimers observed under different conditions.	5
Figure S3. Regional characterization of MMEJ DNA sample.	6
Figure S4. Representative HS-AFM images of MMEJ sample observed in the presence of 1 mM dNTPs and 10 mM Mg ²⁺ .	7
Figure S5. Time-lapse HS-AFM images of a G2L4 RT dimer clamping at MH of a MMEJ dimer.	7
Figure S6. G2L4 RT dimer bound to MMEJ substrate with a topological extrusion of RT3a domain.	8
Figure S7. Representative HS-AFM images of G2L4 RT dimer with different number of RT3a plug protrusion.	9
Figure S8. Representative HS-AFM image of G2L4 RT pre-incubated with MMEJ sample with dNTPs and Mn ²⁺ for one hour.	9
Figure S9. G2L4 monomer can bridge MH formation in the presence of Mn ²⁺ .	10
Figure S10. Structure characterization of MMEJ dimers under different conditions.	10
Figure S11. Terminal transferase activity of G2L4 RT in the presence of Mn ²⁺ and dNTPs.	11

Description of Supplementary Movies

	12
--	----

46 **Materials and Methods**

47 **G2L4 RT Expression and Purification**

48 N-terminal MBP-tagged G2L4 RT was expressed and purified as described.¹ Protein purity
49 is polished by SEC and checked by SDS-PAGE. Protein is concentrated to 8-10mg/ml in 20 mM
50 Tris-HCl pH 7.5, 50 mM NaCl and 10% glycerol and stored at -80°C until used.

51

52 **Factor Xa Cleavage of the N-terminal MBP Tag**

53 To prepare G2L4 RT for HS-AFM experiments, the N-terminal MBP tag was removed by
54 Factor Xa as previously described.¹ Following cleavage, the protein sample was purified using
55 MBP affinity column and checked by SDS-PAGE. The protein was diluted to 1-2 mg/mL in buffer
56 containing 20 mM Tris-HCl pH 7.5, 50 mM NaCl and 10% glycerol at 4°C and stored at -80°C until
57 used.

58

59 **MMEJ Substrate Preparation**

60 MMEJ substrate was prepared by annealing a 96-nt DNA oligonucleotide (Top) ending
61 with a 4-nt microhomology (CCGG) to a complementary 60-nt DNA oligonucleotide with a 3'
62 inverted dT blocking group (Bottom) leaving a 36-nt single-stranded 3' overhang. To anneal the
63 complementary strands of the MMEJ substrate, 10 μ M Top and 20 μ M Bottom oligonucleotides
64 in 100 μ L TE buffer were heated to 95°C for 3 min and cooled at 0.1°C/min to 25°C in a T100
65 thermal cycler (Bio-Rad). Both DNA oligonucleotides were purchased from Integrated DNA
66 Technologies (IDT) and DNA sequences are listed in **Table S1**.

67

68 **HS-AFM Imaging**

69 All HS-AFM movies were taken by amplitude-modulation mode HS-AFM (RIBM, Japan)
70 and imaged in the buffer solutions. Ultrashort Cantilevers (NanoWorld) with a spring constant of
71 \sim 0.15 N/m, resonance frequency of \sim 600 kHz, and a quality factor of \sim 1.5 in buffer solutions were
72 used.

73 Experimental conditions of HS-AFM experiments are summarized in **Table S2**. The
74 imaging buffer for all experiments contained 20 mM Tris-HCl (pH 7.5), 50 mM NaCl and 10 mM
75 MgCl₂, supplemented with MnCl₂, dNTPs and ATP as specified in **Table S2**. To deposit the
76 sample on substrate for imaging, the freshly cleaved mica was pre-incubated with 0.05% (v/v)
77 APTES, and then gently rinsed with Milli-Q water. A total of 1-2 μ L of premixed sample was diluted
78 to proper concentration and deposited on APTES-treated mica surface for 5 mins, gently rinsed
79 with the imaging buffer prior to HS-AFM experiments.

80

81 **Image Processing and Data Analysis**

82 All HS-AFM images were processed in ImageJ with drift correction, background flattening,
83 scanning noise removal, and contrast adjustment. The volume of G2L4 RT particles was analyzed
84 using Gwyddion by properly thresholding the HS-AFM images and measuring grains properties.
85 Simulated AFM images (4 pixels/nm resolution) were generated using Mat-SimAFM² by
86 convolving the protein's PDB structure by a cone-shape tip (tip radius 1 nm, cone angle 15°).
87 Kymographs were generated in ImageJ by reslicing the HS-AFM movies along the DNA
88 backbone, followed by a maximum intensity Z-projection to visualize protein position over time.
89 Intermolecular distances between G2L4 monomers were calculated from the x, y coordinates of
90 protein centers. Protein particles were detected using Laplacian of Gaussian (LoG) detector, and
91 the center coordinates were extracted using Trackmate plugin in Fiji.³ Finally, all data analysis
92 were plotted using custom-written Python scripts.

93

94

95

96 **References:**

- 97 1. Park, S.K. et al. Structural basis for the evolution of a domesticated group II intron-
98 like reverse transcriptase to function in host cell DNA repair. *Proceedings of the*
99 *National Academy of Sciences* **122**, e2504208122 (2025).
- 100 2. Heath, G.R., Micklethwaite, E. & Storer, T.M. NanoLocz: Image Analysis Platform for
101 AFM, High-Speed AFM, and Localization AFM. *Small Methods* **8**, 2301766 (2024).
- 102 3. Ershov, D. et al. TrackMate 7: integrating state-of-the-art segmentation algorithms
103 into tracking pipelines. *Nature Methods* **19**, 829–832 (2022).
- 104

105 **Supplementary Tables**

106
107 **Table S1. MMEJ substrate sequence**
108

Name	Sequence
96-nt DNA 4 microhomology (CCGG) Top	5'CCCTGTACAGTAAGAGCCTACTCATGGATCCTCCTTGTG ATGTAAGGTACAGTAAGATGTGCCTACTCATGGTCGGATC CTCCTTGTGATGCCCGG 3'
60-nt DNA 3' block (Inverted dT at the 3'-end) Bottom	5'ACATCTTACTGTACCTTACATCACAAAGGAGGATCCATGA GTAGGCTCTTACTGTACAGGG/ InvdT / 3'

109
110
111
112
113 **Table S2. Experimental conditions of HS-AFM experiments**
114

Figures	System	Molecular Players			Imaging Buffer				Mixing Molecular Players	
		G2L4	MMEJ	T4 ligase	Mg ²⁺	Mn ²⁺	dNTPs	ATP	Pre-incubation	Live addition
1B(i), 1C(i), 1D, S1	G2L4-APO	50 nM			10 mM					
1B(ii), 1C(ii)	G2L4-Mn ²⁺	50 nM			10 mM	5 mM				
2, S2, S3, S4	MMEJ		10 nM		10 mM					
3A, 3B, S5, S6, S7	G2L4+MMEJ	500 nM	50 nM		10 mM				30 mins~ 2 h	
3C, 3D, 3G, S8, S9	G2L4 repair	500 nM	50 nM		10 mM	1 mM	1 mM			√
3E, 3F, 3H	G2L4 repair	500 nM	10 nM		10 mM	1 mM	1 mM		6 h	
4A	G2L4 repair-molar ratio 10:1	100 nM	10 nM		10 mM	1 mM	1 mM		6 h	
4A	G2L4 repair-molar ratio 50:1	500 nM	10 nM		10 mM	1 mM	1 mM		6 h	
4C, 4E, 4F, 4G, S10	G2L4 repair-elongated and branched products	500 nM	10 nM		10 mM	1 mM	1 mM		6 h	
5	DNA ligation	500 nM	50 nM	0.04 U	10 mM	1 mM	1 mM	1 mM	6 h(repair) Overnight (ligation)	

115

116

117 **Supplementary Figures**

118

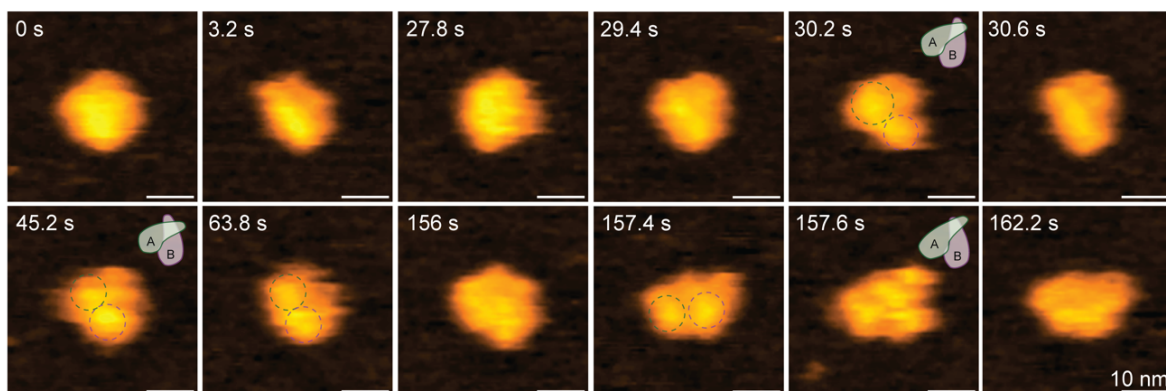


Figure S1. Structural dynamics of a G2L4 RT dimer in APO condition. Representative HS-AFM images of a G2L4 RT dimer show certain conformational dynamics with bi-lobed features (**Movie S2**). At 30.2 s and 45.2 s, the observed structures adopt a dimeric conformation similar to the crystal structure (**Fig. 1D**). At 30.2 s, 45.2s, 63.8 s, and 157.4 s, two palm-finger domains (bi-lobed features, dashed circles) appear slightly separated in a side-by-side arrangement. More fine structural features of G2L4 RT dimer are observed at 157.6 s.

119

120

121

122

123

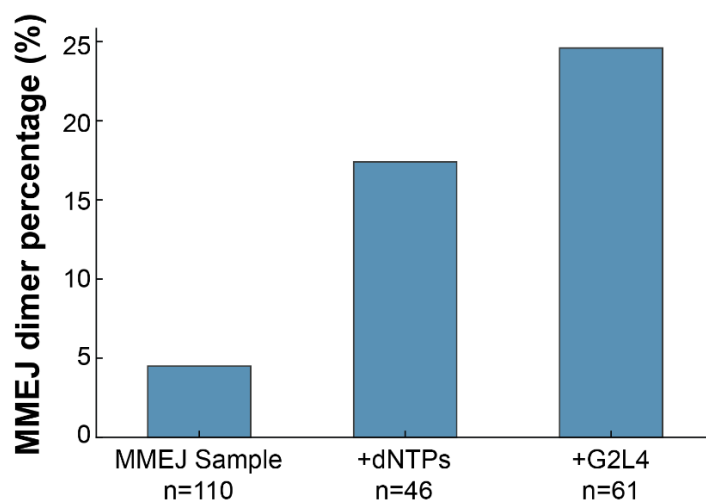


Figure S2. Relative percentage of MMEJ dimers observed under different conditions.

124

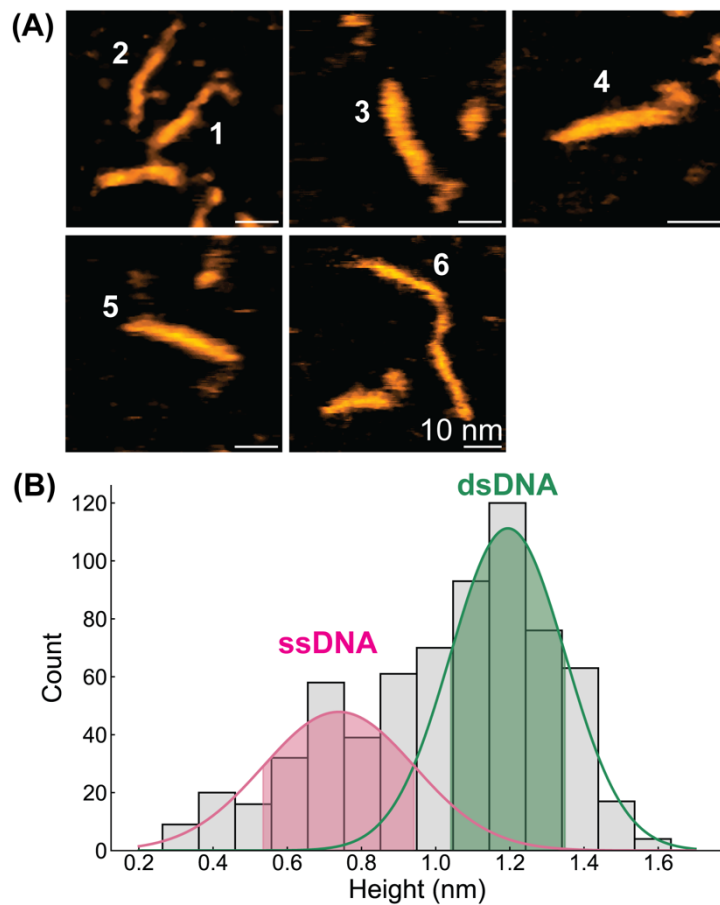


Figure S3. Regional characterization of MMEJ DNA sample. (A) Representative HS-AFM image of MMEJ substrates used to analyze the regions of ssDNA and dsDNA. (B) Accumulative height histograms of the MMEJ substrates masking with a height threshold of 0.3 nm. Two Gaussian fits centered at 0.7 ± 0.2 nm for ssDNA and 1.2 ± 0.2 nm for dsDNA. We note that the mica background is flattened with a mean value of approximately at 0 in height.

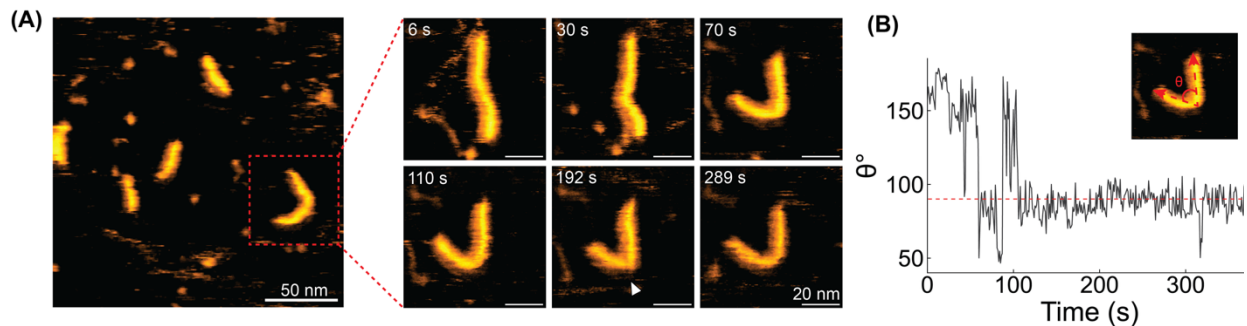


Figure S4. Representative HS-AFM images of MMEJ sample observed in the presence of 1 mM dNTPs and 10 mM Mg^{2+} . (A) Time-lapse HS-AFM images of a MMEJ dimer without dissociation. The sharp bend, indicated by white arrowhead, highlights the DSBR is incomplete purely with dNTPs filling up the ss-gaps. (B) Tracked bending angle between two ends of the observed MMEJ dimer. Red dashed line represents 90 degrees.

126
127
128
129

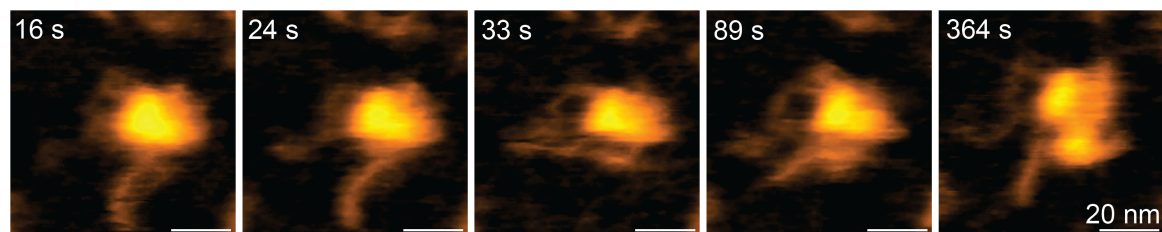


Figure S5. Time-lapse HS-AFM images of a G2L4 RT dimer clamping at MH of a MMEJ dimer. Although the G2L4 RT dimer shows certain conformational changes, the protein-DNA complex remains stable during the observation.

130

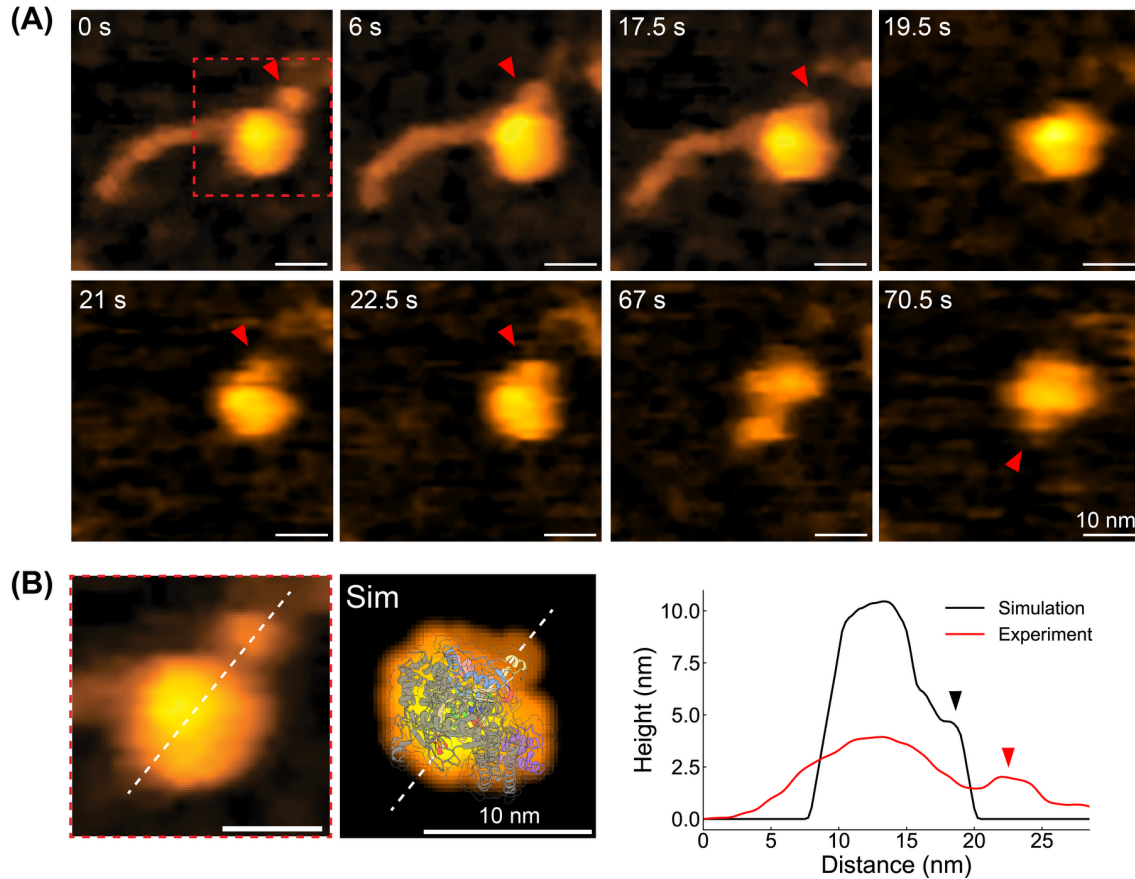


Figure S6. G2L4 RT dimer bound to MMEJ substrate with a topological extrusion of RT3a domain. (A) Representative HS-AFM images showing a small RT3a plug protrusion (red arrows) when G2L4 RT dimer binds to MMEJ substrate. (B) The comparison between zoomed-in HS-AFM image of the G2L4 RT dimer and simulated AFM topography of G2L4 RT dimer in complex with 15-nt snapback substrate (PDB: 9D4S; molecular orientation is adjusted and viewed from the side to highlight RT3a plug). Right: Height cross-sectional profile of the experimental and simulated AFM data along the white dashed lines. The arrows indicate the position of RT3a plug. The significant height difference between experimental and simulated AFM data is due to the G2L4 RT is free-standing above the background substrate in simulated AFM topography.

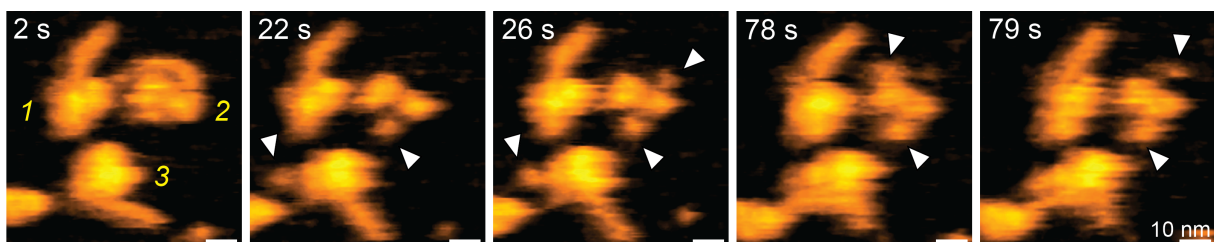


Figure S7. Representative HS-AFM images of G2L4 RT dimer with different number of RT3a plug protrusion. Three G2L4 RT dimers, highlighted by yellow numbers, individually bind to a MMEJ substrate ($t = 2$ s). For G2L4 RT#2, the MMEJ substrate dissociates from this protein with a bi-lobed feature, where two RT3a plug extrusions are observed at the opposite sides, indicated white arrows.

132
133

134

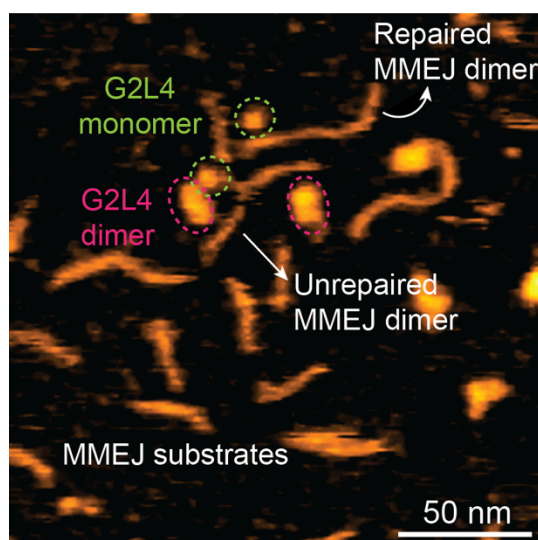


Figure S8. Representative HS-AFM image of G2L4 RT pre-incubated with MMEJ sample with dNTPs and Mn^{2+} for one hour. G2L4 monomers, dimers, and both repaired and unrepaired MMEJ dimers are coexisted.

135

136

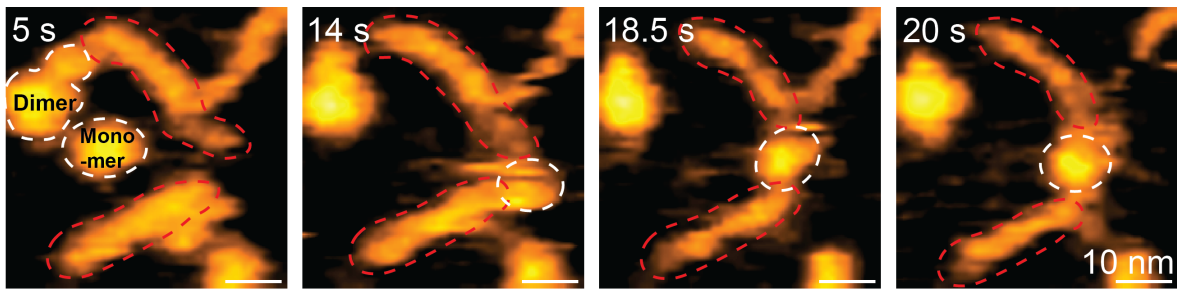


Figure S9. G2L4 monomer can bridge MH formation in the presence of Mn^{2+} . At $t = 5$ s, two MMEJ substrates are separated as highlighting by red dashed circles. After 14 s, a G2L4 monomer bridged two ss-DNA overhangs together, forming MH.

137

138

139

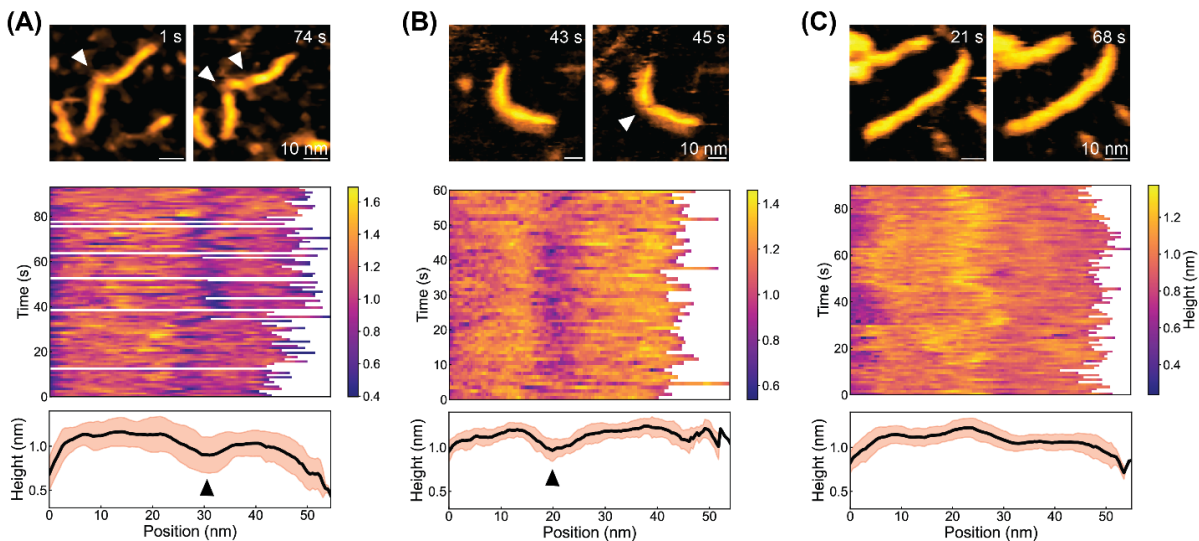


Figure S10. Structure characterization of MMEJ dimers under different conditions. Each panel displays (*top*) representative HS-AFM images, (*middle*) kymographs of height along the DNA backbone, and (*bottom*) average height profile (solid black line) with standard deviation, orange shading, for (A) MMEJ sample alone, (B) MMEJ sample incubated with dNTPs, and (C) MMEJ dimer incubated with G2L4 RT, dNTPs and Mn^{2+} .

140

141

142

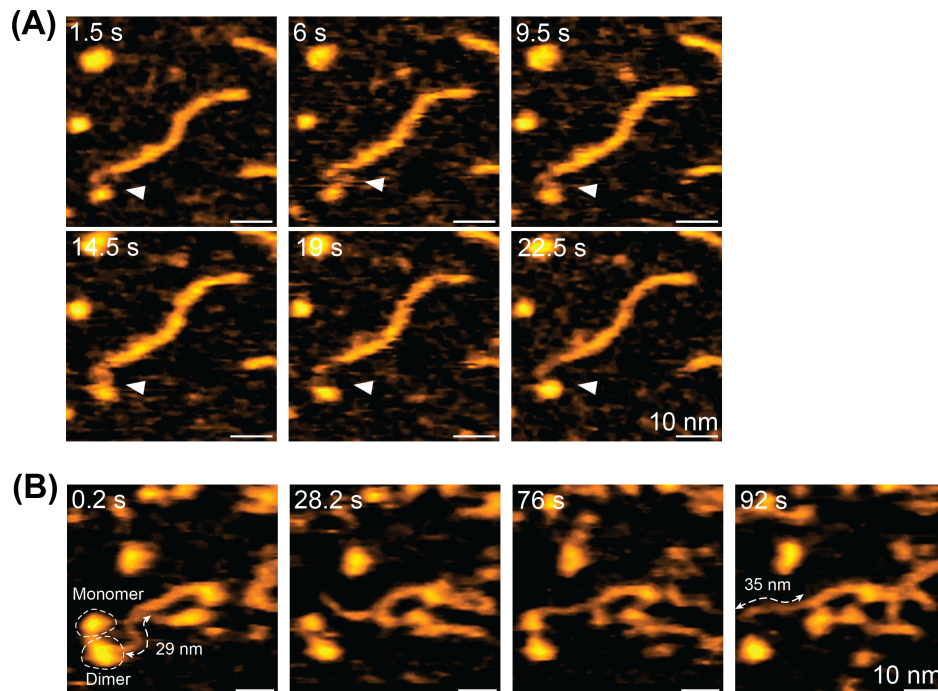


Figure S11. Terminal transferase activity of G2L4 RT in the presence of Mn^{2+} and dNTPs. **(A)** Time-lapse HS-AFM images of a G2L4 RT monomer interacting with ssDNA overhang, indicated by white arrowheads. No significant elongation is observed in the trajectory. **(B)** Realtime ssDNA elongation by G2L4 RT molecules. The ssDNA length is measured by setting high threshold at 0.8 nm, and increased by ~ 6 nm (~ 30 nt; by assuming 0.2 nm/nt obtained in **Fig. 2C**) at 92 s.

144 **Description of Supplementary Movies**

145 **Supplementary Movie S1. Structural dynamics of APO-G2L4 RT dimer.** HS-AFM movie of an
146 APO-G2L4 RT dimer deposited on freshly cleaved mica (see **Fig. 1C-(i)**). The G2L4 RT molecule
147 was aligned at the center for enhancing the conformational dynamics. Imaging parameters: 2
148 frames/s, 0.25 nm/pixel.

149
150 **Supplementary Movie S2. Structural dynamics of another APO-G2L4 RT dimer.** HS-AFM
151 movie of another APO-G2L4 RT dimer deposited on freshly cleaved mica (see **Fig. 1D** and **Fig.**
152 **S1**). Imaging parameters: 5 frames/s, 0.5 nm/pixel.

153
154 **Supplementary Movie S3. Dissociation of a G2L4 dimer in Mn²⁺ condition.** HS-AFM movie
155 of a G2L4 RT dimer observed in buffer containing 6 mM Mn²⁺ (see **Fig. 1C-(ii)**). At the beginning
156 of the movie (~1 s), a monomer and a dimer coexisted in the imaging area. The dimer was intact
157 at ~13 s and then began showing conformational changes with two lobed-like structure
158 occasionally visible. Two monomers fully dissociated at ~182 s. Imaging parameters: 1 frame/s,
159 0.375 nm/pixel.

160
161 **Supplementary Movie S4. Structural dynamics of individual MMEJ substrates.** HS-AFM
162 movie of three individual MMEJ substrates deposited on APTES-coated mica (see **Fig. 2B**). The
163 MMEJ substrates, especially the middle one, showed clear height difference along the DNA
164 backbone, indicating the regions of dsDNA and ssDNA. ssDNA overhang was more flexible
165 compared to dsDNA end. Imaging parameters: 1 frame/s, 0.5 nm/pixel.

166
167 **Supplementary Movie S5. Structural dynamics of a MMEJ dimer.** HS-AFM movie of a MMEJ
168 dimer deposited on APTES-pretreated mica (see **Fig. 2D**). The MH region and ss-gap could be
169 clearly identified by the height variation along the backbone. The dsDNA region was freely rotating
170 as an arm relative to the ss-gap as a hinge. Imaging parameters: 1 frame/s, 0.5 nm/pixel.

171
172 **Supplementary Movie S6. Association and dissociation of a MMEJ dimer.** HS-AFM movie of
173 realtime association and dissociation of a MMEJ dimer (see **Fig. 2E**). In this scanning area, there
174 initially were a MMEJ substrate and a transiently formed MMEJ dimer. In the absence of G2L4
175 RT, the MH dissociated at ~3.5 s, associated again at ~4 s, and finally separated after 6 s. Imaging
176 parameters: 2 frames/s, 0.286 nm/pixel.

177
178 **Supplementary Movie S7. A MMEJ dimer clamped by a G2L4 RT dimer.** HS-AFM movie of a
179 G2L4 dimer clamping at the MH region between two MMEJ substrates (see **Fig. S5**). Imaging
180 parameters: 1 frame/s, 0.5 nm/pixel.

181
182 **Supplementary Movie S8. G2L4 RT dimer with a RT3a plug protrusion upon MMEJ**
183 **substrate engagement.** HS-AFM movie showing a small RT3a plug protrusion when G2L4 RT
184 dimer binds to MMEJ substrate (see **Fig. 3B** & **Fig. S6**). Imaging parameters: 2 frames/s, 1
185 nm/pixel.

186
187 **Supplementary Movie S9. G2L4 RT dimer repositions on a MMEJ dimer.** HS-AFM movie of
188 a G2L4 RT dimer repositioning on a MMEJ dimer (see **Fig. 3C**). The imaging was performed on
189 0.05% APTES coated mica, with repair reaction mixture added realtime into liquid cell. The G2L4
190 RT dimer was firstly bound to the right ss-gap, repositioned to the left ss-gap (~37 s), bounced
191 back and forth twice, and finally bound to the left ss-gap. At 94 s, another G2L4 RT dimer bound
192 to the left side of DNA. Imaging parameters: 2 frames/s, 1 nm/pixel.

193

194 **Supplementary Movie S10. Molecular interactions between G2L4 RT and long DNA**
195 **products.** HS-AFM movie of an intermediate DNA product interacting with several G2L4 RT
196 molecules (see **Fig. 4E**). Along the DNA backbone, three events were happening simultaneously:
197 G2L4 dimer sliding, unidirectional repair and strand annealing. Imaging parameters: 1 frame/s,
198 1.5 nm/pixel.
199

200 **Supplementary Movie S11. Self-rearrangements of the DNA backbone at a nicked site to**
201 **form a branched morphology.** HS-AFM movie of an intermediate DNA product showing strand
202 rearrangement (see **Fig. 4H**). The long linear DNA product was broken at a nicked site (~93 s).
203 The broken end rearranged to the middle of DNA backbone, forming a branched structure.
204 Imaging parameters: 1 frame/s, 1 nm/pixel.
205

206 **Supplementary Movie S12. T4 DNA ligase repairs a MMEJ dimer.** HS-AFM movie of a T4
207 DNA ligase interacting with a MMEJ dimer with a nick site (see **Fig. 5D-5E**). A T4 DNA ligase in
208 solution appeared to bind to the MMEJ dimer (~23 s). The DBD domain initiated the DNA
209 engagement, slid to search nick site (23~27 s). After transient domain rearrangement (28~29 s),
210 the DNA backbone is ligated after 38 s. Imaging parameters: 1 frame/s, 0.25 nm/pixel.
211
212